

# A biocomposite of collagen nanofibers and nanohydroxyapatite for bone regeneration

Nilza Ribeiro, Susana R Sousa, Clemens A van Blitterswijk, Lorenzo Moroni and Fernando J Monteiro

## Abstract

This work aims to design a synthetic construct that mimics the natural bone extracellular matrix through innovative approaches based on simultaneous type I collagen electrospinning and nanophased hydroxyapatite (nanoHA) electrospraying using non-denaturing conditions and non-toxic reagents. The morphological results, assessed using scanning electron microscopy and atomic force microscopy (AFM), showed a mesh of collagen nanofibers embedded with crystals of HA with fiber diameters within the nanometer range (30 nm), thus significantly lower than those reported in the literature, over 200 nm. The mechanical properties, assessed by nanoindentation using AFM, exhibited elastic moduli between 0.3 and 2 GPa. Fourier transformed infrared spectrometry confirmed the collagenous integrity as well as the presence of nanoHA in the composite. The network architecture allows cell access to both collagen nanofibers and HA crystals as in the natural bone environment. The inclusion of nanoHA agglomerates by electrospraying in type I collagen nanofibers improved the adhesion and metabolic activity of MC3T3-E1 osteoblasts. This new nanostructured collagen–nanoHA composite holds great potential for healing bone defects or as a functional membrane for guided bone tissue regeneration and in treating bone diseases.

**Keywords:** biocomposite, collagen nanofibers, nanohydroxyapatite, electrospinning, electrospraying

---

## 1. Introduction

Considerable attempts have been made to produce adequate matrices or scaffolds that mimic the bone extracellular matrix (ECM) for applications in tissue engineering and regenerative medicine. These biomaterials should be specifically designed to be biocompatible, biodegradable and osteoconductive. Nanohydroxyapatite/collagen nanocomposites are ideal biomaterials for bone regeneration and target molecule delivery

systems for the treatment of bone diseases. These types of biomaterials are suitable for bone contact and substitution, particularly novel natural polymer-based composites reinforced with bioactive components, such as nanophased hydroxyapatite (nanoHA) [1–5]. They represent the major inorganic and organic component assembly as in natural bone where the HA crystals of the mineral part are bound to collagen fibers, corresponding to 90–95 per cent of the bone organic matrix. The mineral phase is responsible for

providing adequate mechanical compressive strength, while collagen provides tensile properties.

Electrospinning has recently attracted great interest in generating nanoscale fibers of biomaterials ranging from polymers and ceramics to their composite fibrous scaffolds for tissue engineering applications with fiber diameters ranging from a few microns to less than 100 nm [6, 7]. This type of nanofibrous structure is regarded as a promising architecture in the sense that natural bone ECM exhibits collagen fibrils with diameters ranging from 20 nm to 40  $\mu\text{m}$  [8, 9] which are far smaller than those that can be achieved with conventional processing methods.

Natural polymers, including collagen, are very difficult to electrospin due to their high viscosity and low solubility in general organic solvents, as reported in most published works concerning the production of collagen fibrillar meshes [10–19]. For that reason, synthetic polymers such as polyglycolic acid (PGA), polyL-lactic acid (PLLA), polylactide-co-glycolic acid (PLGA) or polycaprolactone (PCL) are often added to the collagen solution [20–22]. However, the chemicals (additives, traces of catalysts, inhibitors) or monomers (glycolic acid, lactic acid) released from polymer degradation may induce local and systemic host reactions that may cause clinical problems [23, 24]. Another way to overcome this problem is the use of organic toxic reagents, mainly highly volatile fluoroalcohols such as 1,1,1,3,3,3-hexafluoro-2-propanol (HFP) and 2,2,2-trifluoroethanol (TFE). However, these solvents are highly toxic and partially denature the native structure of collagen through the disruption of its characteristic triple-helical structure, decrease its denaturation temperature and result in a significant amount of collagen lost during electrospinning [25, 26]. Increasing efforts towards applying non-toxic aqueous systems, such as PBS/ethanol or acetic acid, for medical applications have started to emerge [27–30]. In addition, post-fabrication cross-linking confers mechanical resistance through the binding of carboxylic groups in collagen fibrils, which is fundamental for *in vitro* assays and

translation of these collagenous meshes in preclinical and clinical settings. In this work, we used N-ethyl-N'-[3-dimethylaminopropyl] carbodiimide/N-hydroxy succinimide (EDC/NHS) as a non-toxic cross-linker, despite most of the studies in the literature having applied toxic reagents such as glutaraldehyde [27, 31–35].

Here, we report an innovative approach based on two simultaneous methods, type I collagen electrospinning and nanophased HA electrospaying, using non-toxic reagents. Simultaneous electrospinning and electrospaying techniques have been applied to gelatin in only very few studies [36, 37]. The physicochemical properties of this biocomposite were investigated as well as its influence on MC3T3-E1 osteoblast cell performance in terms of morphology, adhesion and metabolic activity. This construct is revealed to have a non-cytotoxic effect and the ability to support osteoblast cell adhesion and viability.

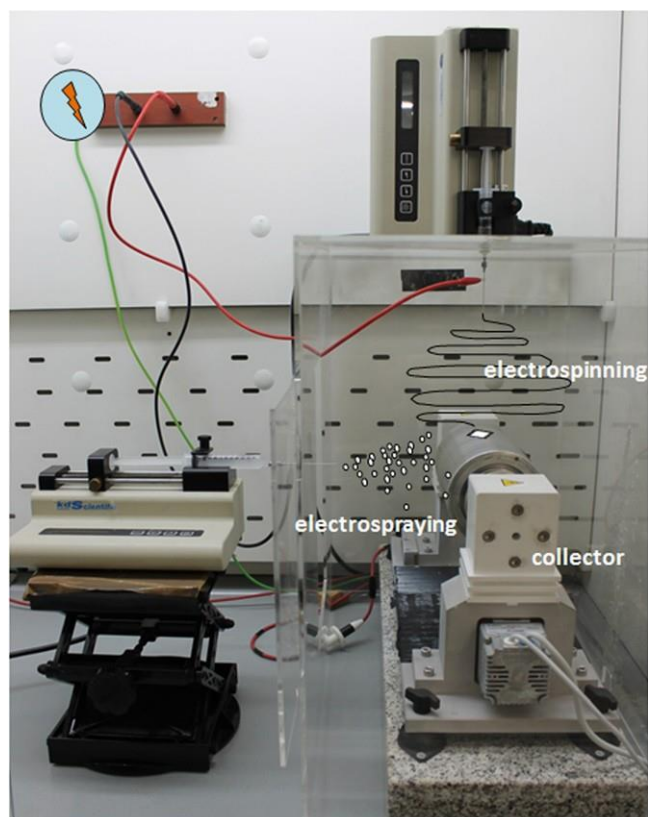


Figure 1. A schematic diagram of the laboratory set-up used for the simultaneous electrospinning and electrospaying techniques.

## 2. Materials and methods

### 2.1. Electrospinning and electrospaying

Type I collagen, supplied by Kensey Nash (USA), was suspended in acetic acid:ethyl acetate:water (40:30:30) by stirring overnight at 4 °C to obtain a 12% ( $\text{w v}^{-1}$ ) collagen suspension. The solution was loaded into a syringe (5 ml) with a 21 G needle and electrospun at 0.1  $\text{ml h}^{-1}$ , under a high electrostatic field (20 kV) onto 12 mm diameter coverglasses attached on aluminum foil wrapped on a rotating cylinder collector, at 400 rpm, placed at a distance of 120 mm from the needle tip. Simultaneously, electrospaying of nanoHA, supplied by Fluidinova S.A. (Portugal), (nanoXIM-Hap102), was carried out. NanoHA 3.5% ( $\text{v v}^{-1}$ ) suspended in methanol was subjected to a set of ultrasonic cycles with an amplitude of 60 A ( $20 \times 15$  ultrasonic pulses) in order to decrease nanoparticle agglomeration. The solution was loaded into a syringe (10 ml) with a 21 G needle and electrospayed at 2  $\text{ml h}^{-1}$ , under a high electrostatic field (20 kV) onto the collagen fibers at a distance of 120 mm. The simultaneous electrospinning and electrospaying process was continuously performed over 1 h at room temperature (22 °C) with a relative humidity of about 30–45%. Figure 1 illustrates the schematic diagram of the laboratory set-up used for the simultaneous electrospinning of collagen and electrospaying of nanoHA techniques. The samples obtained were subjected to chemical cross-linking in ethanol 90% ( $\text{v v}^{-1}$ ) containing

20 mM EDC and 10 mM NHS at 4 °C over 4 h in the case of the electrospun collagen fibers and 24 h in the case of the electrospun collagen fibers plus electrospayed HA agglomerates. EDC, a zero-length cross-linker, causes a direct conjugation of carboxylates (–COOH) to primary amines (–NH<sub>2</sub>) without becoming part of the final cross-link (amide bond) between the target molecules. The cross-linked constructs were washed three times with ethanol 90% (v v<sup>-1</sup>) and twice with water and dried overnight at room temperature in a desiccator before chemical and morphological characterization and cell culture studies. All the experimental conditions related to the weight % ratio of collagen–nanoHA, the proportion of reagents and the electrospinning/electrospraying conditions referred to previously were optimized in order to produce a stable network of collagen nanofibers and HA agglomerates (data not shown).

## 2.2. Substrate characterization

The size of the HA agglomerates was determined using a Zetasizer Nano ZS (Malvern Instruments, U.K.), equipped with a 4 mW HeNe laser beam with a wavelength of 633 nm and a scattering angle of 173°. The size measurements were performed following the manufacturer's instructions, at 25 °C in a polystyrene cell (ZEN0040), using the 'General Mode' analysis model, which is suitable for the analysis of the majority of samples and dispersions. Size results were automatically calculated by the software, DTS Nano v.6.30, using the Stokes–Einstein equation.

Chemical characterization of the developed structures was performed using Fourier transformed infrared spectroscopy (FT-IR), with a Perkin-Elmer 2000 FT-IR spectrometer. For this purpose, 0.2 g of sample material (collagen, electrospun collagen fibers or composites of collagen and nanoHA obtained by simultaneous electrospinning and electrospraying) was ground and analyzed as KBr pellets at a spectral resolution of 4 cm<sup>-1</sup>. One hundred scans were accumulated per sample.

The proportion of collagen and nanohydroxyapatite present in the composites was assessed by Thermogravimetric analysis (TGA) using a NETZSCH simultaneous thermal analysis (STA) 449 F3 Jupiter® instrument. Approximately 4.4 mg of sample was placed in an alumina sample crucible and heated at 10 °C min<sup>-1</sup> from 25 °C to 500 °C, under nitrogen atmosphere with a flow rate of 30 ml min<sup>-1</sup>.

The surface characterization of substrates was examined using scanning electron microscopy (SEM). SEM analyses were performed using a FEI Quanta 400FEG/EDAX Genesis X4M (Hillsboro, OR, USA) scanning electron microscope under high vacuum conditions. The samples were sputter-coated with a thin palladium–gold film, using a sputter coater (SPI-Module) in an argon atmosphere before observation. The diameters of twenty fibers randomly chosen from six different SEM images, each one corresponding to a distinct sample, were measured with a custom code image analysis implemented in the program ImageJ. The results referred to as diameter measurements correspond to the average and median ± standard deviation (SD). The thicknesses of the

collagen–HA biocomposites before and after chemical cross-linking were obtained through SEM image analysis. For both conditions, each sample ( $n = 4$ ) was placed in a container with liquid N<sub>2</sub> and then a free fracture was produced under low temperature. The exposed fracture was observed by SEM under high vacuum, and images were produced with secondary electrons. For each sample, a total of four measurements were taken randomly. The results referred to as thickness measurements correspond to the average ± standard deviation (SD).

Atomic force microscopy (AFM) studies were carried out using a Veeco Multimode NanoScope IVa scanning probe microscope. The surface topography of the collagen–nanoHA composite was imaged with a 16 × 16 μm<sup>2</sup> piezo-scanner. Imaging analyses were performed at room temperature, in Tapping mode®, using a silicon cantilever with a spring constant of 25–75 N m<sup>-1</sup> (tip radius <10 nm). The mechanical properties of electrospun ultra-thin non-woven collagen fiber mats before and after chemical cross-linking were determined by nanoindentation using a diamond-tipped probe cantilever with a resonance frequency of 60 kHz and a nominal spring constant of 131.0 N m<sup>-1</sup> (DNISP; Veeco Probe, United States). For each sample, a total of 16 nanoindentations were taken randomly. The time for both approach and retraction of the tip was set to 1.7 s (1/0.6 Hz), with zero delay in between and a maximum load of 3 μN. All the measurements were taken in air and at room temperature. The Oliver and Pharr indentation model was applied to each load–unload curve, in order to obtain the elastic modulus or Young's modulus parameter ( $E$ ) [38]. For the calculations we assumed a Poisson coefficient of 0.2 for the collagen material (in fact, this model is not highly dependent on this coefficient). All calculations were performed using NanoScope v6.13 software.

## 2.3. In vitro cell culture studies

MC3T3-E1 cells, established as an osteoblastic cell line from normal mouse calvaria, were grown in an alpha minimum essential medium (α-MEM, Gibco) supplemented with 10% (v v<sup>-1</sup>) foetal bovine serum (FBS) (Invitrogen) and 1% penicillin–streptomycin (Gibco). Cells were cultured in 75 cm<sup>2</sup> plastic culture flasks, and incubated in a humidified incubator (37 °C and 5% CO<sub>2</sub>).

Freshly confluent MC3T3-E1 cells were rinsed with PBS, followed by incubation in trypsin/EDTA (0.25% trypsin, 1 mM EDTA; Sigma) for 10 min at 37 °C and then re-suspended in supplemented medium. The substrates were sterilized by immersion in a series of dilute ethanol solutions of 90, 70 and 50% (v v<sup>-1</sup>) over 10 min, and incubated with α-MEM for 30 min. After rinsing three times in PBS, the cells were seeded on both substrates (electrospun collagen fibers and collagen–nanoHA composites obtained by co-electrospinning/electrospraying) at a cell seeding density of 4 × 10<sup>4</sup> cells/well. Coverglasses coated with Poly-D-lysine hydrobromide (PDL) were used as a control. MC3T3-E1 cells were cultured on both constructs for periods of 4 h and 1, 4, 7, 14 and 21 days. For each material and culture period, six samples

without cells were incubated with complete medium in the same way and used as blanks.

The cell metabolic activity of MC3T3-E1 cells on substrates after 4 h and 1, 4, 7, 14 and 21 days of cell culture was evaluated using a resazurin-based assay [37]. Thus, 50  $\mu\text{l}$  of resazurin (Sigma) at a concentration of 0.1  $\text{mg ml}^{-1}$  were added to each well. After 3 h of reaction time, 100  $\mu\text{l}$  of supernatant was transferred to the wells of a black-walled 96-well plate. Fluorescence was read using  $\lambda_{\text{ex}}=530\text{ nm}$  and  $\lambda_{\text{em}}=590\text{ nm}$  in a microplate reader (Biotek, Synergy MX). The fluorescence value corresponding to the unseeded substrates was subtracted. The results correspond to the mean  $\pm$  standard deviation of six cultured samples.

The MC3T3-E1 cell distribution and morphology on the materials was assessed using confocal microscopy and SEM. For immunostaining of the F-actin cytoskeleton and nuclei, the cell-seeded surfaces were rinsed twice with PBS and fixed with 4% para-formaldehyde for 15 min. After washing with PBS, cells were permeabilized with 0.1% Triton X-100 for 5 min and incubated in 1% BSA for 30 min at room temperature. Cell cytoskeleton filamentous actin was visualized by treating the cells with Alexa Fluor<sup>®</sup> 594 Phalloidin (1:200 in BSA 1%, Molecular Probes<sup>®</sup>) for 20 min in the dark. Finally the cells were washed with PBS and the cell nuclei were counterstained with 4', 6-diamidino-2-phenylindole (Vectashield/DAPI) dye for 10 min in the dark. The images were acquired on a Leica SP5 confocal microscope (Leica Microsystems, Wetzlar, Germany) using a Plan-Apochromat 63  $\times$  oil objective. Images were processed and quantified using LAS AF v2.6.0.7266 software. Background noise was minimal when the optimal gain/offset settings for the detectors were used. Digital images were optimized for contrast and brightness using Adobe Photoshop (Adobe Systems, San Jose, CA). For the SEM observations, cell-seeded samples fixed with 1.5% glutaraldehyde were dehydrated with an increasing ethanol–water gradient and dried using hexamethyldisilazane. SEM analyses were performed using the same scanning electron microscope equipment described in section 2.2. Samples were sputter-coated with a thin palladium–gold film, using a sputter coater (SPI-Module) in an argon atmosphere before being observed. Samples were collected at days 1, 4, 7, 14 and 21 of MC3T3-E1 culture on the substrates.

Statistical analysis was assessed using one-way ANOVA, with a significance level of  $p \leq 0.05$ . GraphPad version 5.02 software was used to perform the analysis.

### 3. Results and discussion

#### 3.1. Substrate production and chemical–physical properties

Both solubilization and electrospinning procedures have noticeable effects on collagen fiber diameter and morphology, namely, the flow rate, electrospinning voltage, needle and collection distance, and most critically, the concentration of collagen solution and solvent type. Previously, we tried to replicate the experimental conditions reported by the few

published works that applied non-toxic aqueous solvents in the electrospinning of collagen, but without success. This was probably due to a different type I collagen origin and purity, as well as environmental conditions such as relative humidity of air, seldom mentioned and temperature. Hence, the parameters of solubilization and electrospinning were optimized as described in section 2.1, in order to produce continuous collagen nanoscale-diameter fibers, the native structure of which is preserved, from an aqueous solution composed of acetic acid:ethyl acetate:water (40:30:30), embedded with crystals of HA. The addition of ethyl acetate improved the spinnability of the nanofibers and reduced the acidity of the solvent (acetic acid) [39]. Since we wanted to preserve the nanometric scale of the HA agglomerates resulting from the electrospraying technique, a nanoHA gel was used instead of nanoHA powder. This means that the nanoHA did not undergo a spray drying process, which typically enhances the degree of agglomeration of nanoHA particles. Also, the nanoHA solution was subjected to a set of ultrasonic cycles before the electrospraying process. The sizes of the HA agglomerates were assessed by Zetasizer Nano ZS. As expected, there was a steady decrease in size with increasing number of ultrasonic pulses. Comparing the HA agglomerates' size before and after ultrasonic pulse cycles, a reduction in size from  $278 \pm 30\text{ nm}$  to  $126 \pm 2\text{ nm}$  was observed.

The collagenous integrity as well as the presence of nanoHA in the nanostructured collagen–nanoHA composite was confirmed by FT-IR. The spectrum of electrospun collagen nanofibers in figure 2 depicts characteristic absorption bands at 1657, 1536 and 124  $\text{cm}^{-1}$ , attributable to amide I, II and III, respectively. The amide I absorption arises predominantly from protein amide C = O stretching vibrations, amide II is made up of amide N–H bending vibrations and C–N stretching vibrations while amide III arises predominantly from C–N stretching and N–H in-plane bending from amide linkages. The integrity of collagen's triple helix can be evaluated by the ratio between the absorbance at 1235 and 1450  $\text{cm}^{-1}$ . Ratio values for denatured collagen are around 0.5 and those for intact structures are around 1. For the analyzed samples, the value obtained was 1.07, indicating that the addition of nanoHA and the applied conditions did not destabilize the collagen's triple helix. There was no band at 1706  $\text{cm}^{-1}$ , which suggests that there was no free acetic acid in the sample [40, 41]. Furthermore, the FT-IR spectrum of the collagen–nanoHA composites obtained using the simultaneous electrospinning and electrospraying techniques, in addition to the collagen characteristic bands referred to previously, revealed characteristic bands of nanophased HA,  $\text{OH}^-$  vibrational (633  $\text{cm}^{-1}$ ) bands and  $\text{PO}_4$  ( $\nu_3 \sim 1093$  and 1032  $\text{cm}^{-1}$ ;  $\nu_1 \sim 962\text{ cm}^{-1}$ ,  $\nu_4$  601 and 564  $\text{cm}^{-1}$ ) bands. The characteristic bands of the carbonate group can also be observed, namely those corresponding to the  $\nu_3$  vibration of C–O (1452  $\text{cm}^{-1}$ ) and the  $\nu_2$  vibrations (875  $\text{cm}^{-1}$ ) [42].

In order to quantify the amount of organic and inorganic components in the collagen–nanoHA composite, TGA measurements were carried out. TGA curves of the collagen–nanoHA composite showed weight loss in the range from room temperature to 100°C due to the evaporation of

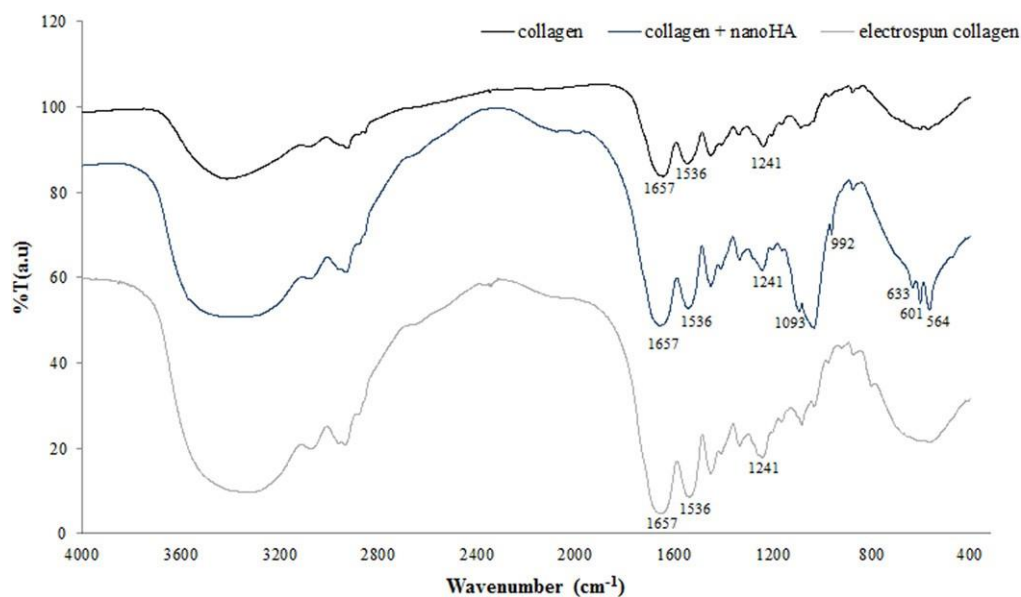


Figure 2. FT-IR spectra of collagen, electrospun collagen and collagen–nanoHA composites obtained using the simultaneous electrospinning and electrospaying techniques.

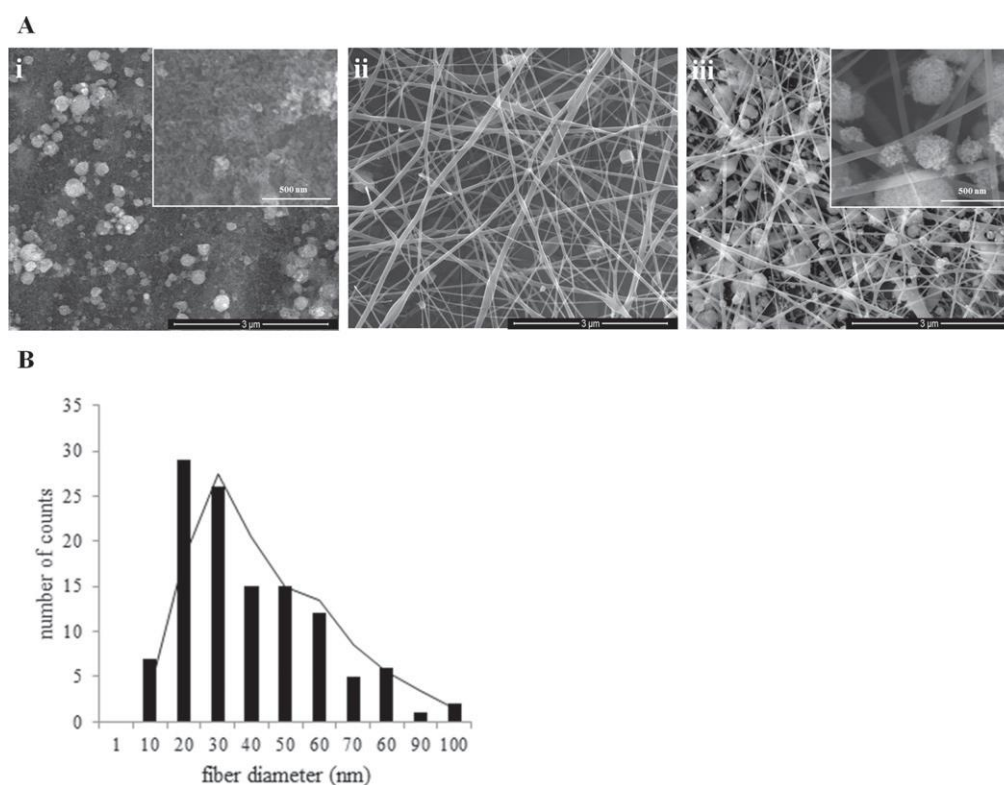


Figure 3. (A) SEM images of electrospayed nanoHA (i), electrospun collagen nanofibers (ii) and collagen–nanoHA composites obtained using the simultaneous electrospinning and electrospaying techniques (iii). (B) A histogram of the electrospun collagen fiber diameter distribution obtained using SEM.

physisorbed water and weight loss between 250 and 500 °C associated with the decomposition of collagen molecules (data not shown). Considering the residual mass values obtained by TGA, the inorganic content in the collagen–HA composite was  $48.14 \pm 0.22$  wt %.

In addition to the Zeta sizer results, the nanometric scale of the nanoHA agglomerates was confirmed using SEM image analysis, (figure 3(A)(i)). The SEM images of the electrospun collagen revealed a random mesh of collagen nanofibers. The diameter measurements of twenty collagen



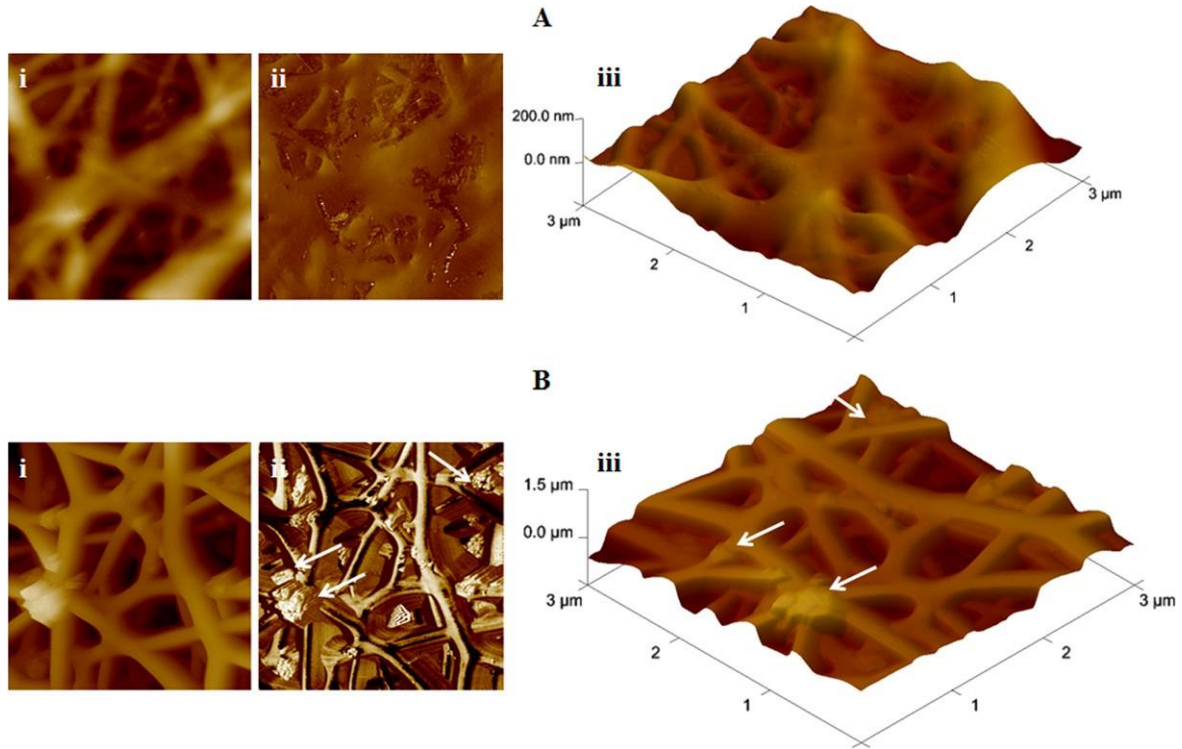


Figure 4. Surface topography of the electrospun collagen nanofibers (A) and the collagen–nanoHA composite (B): height (i), phase (ii) and 3D (iii) images. All AFM images were obtained under Tapping mode® (image scale  $3 \times 3 \mu\text{m}^2$ ). Arrows indicate nanoHA agglomerates.

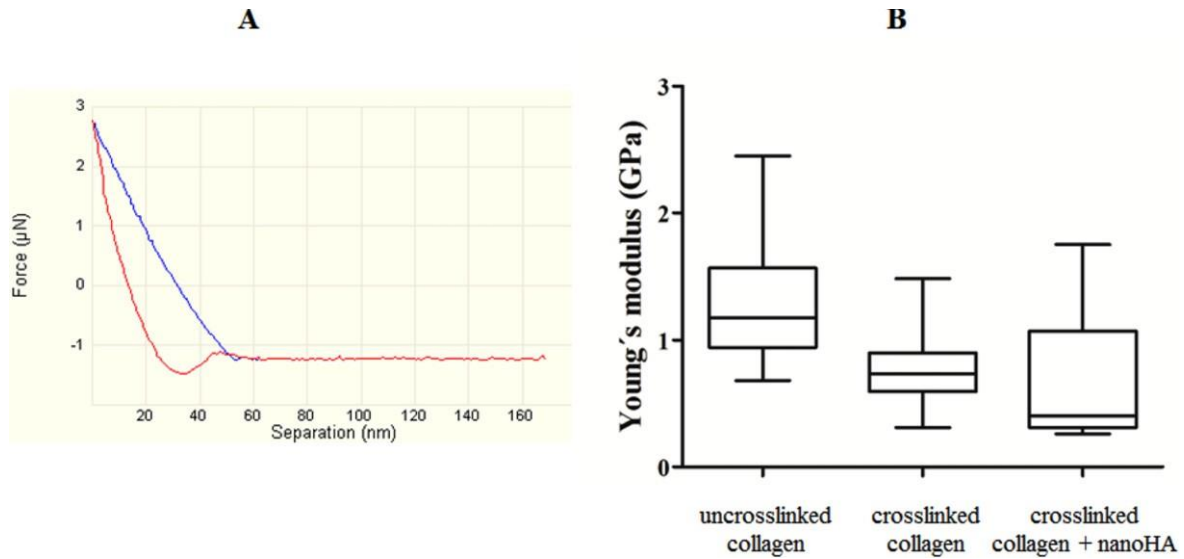


Figure 5. An example of an indentation curve (A) and Young's moduli (B) of uncross-linked collagen nanofibers, cross-linked collagen nanofibers and cross-linked collagen–HA composites obtained by nanoindentation.

fibers randomly chosen from six different SEM images, with a custom code image analysis implemented in the program ImageJ, allowed the calculation of average and median values,  $37.2 \pm 23.2 \text{ nm}$  and  $30.2 \pm 23.2 \text{ nm}$ , respectively (figure 3(B)). These diameter values are within the nanometer range and are significantly lower than those reported in the literature, which typically exceed  $200 \text{ nm}$  [14, 21]. It is interesting to note that collagen fibers obtained by

electrospinning using organic toxic solvents the diameters of which are in the micrometer scale are often called collagen nanofibers, although in reality they are far beyond the nanometer scale. In addition, their diameters are substantially higher than the collagen nanofibers produced by electrospinning using acetic acid as the solvent and a low protein concentration as in our work or in Liu's work [10, 13, 15, 17, 29]. In conclusion, the reason why the

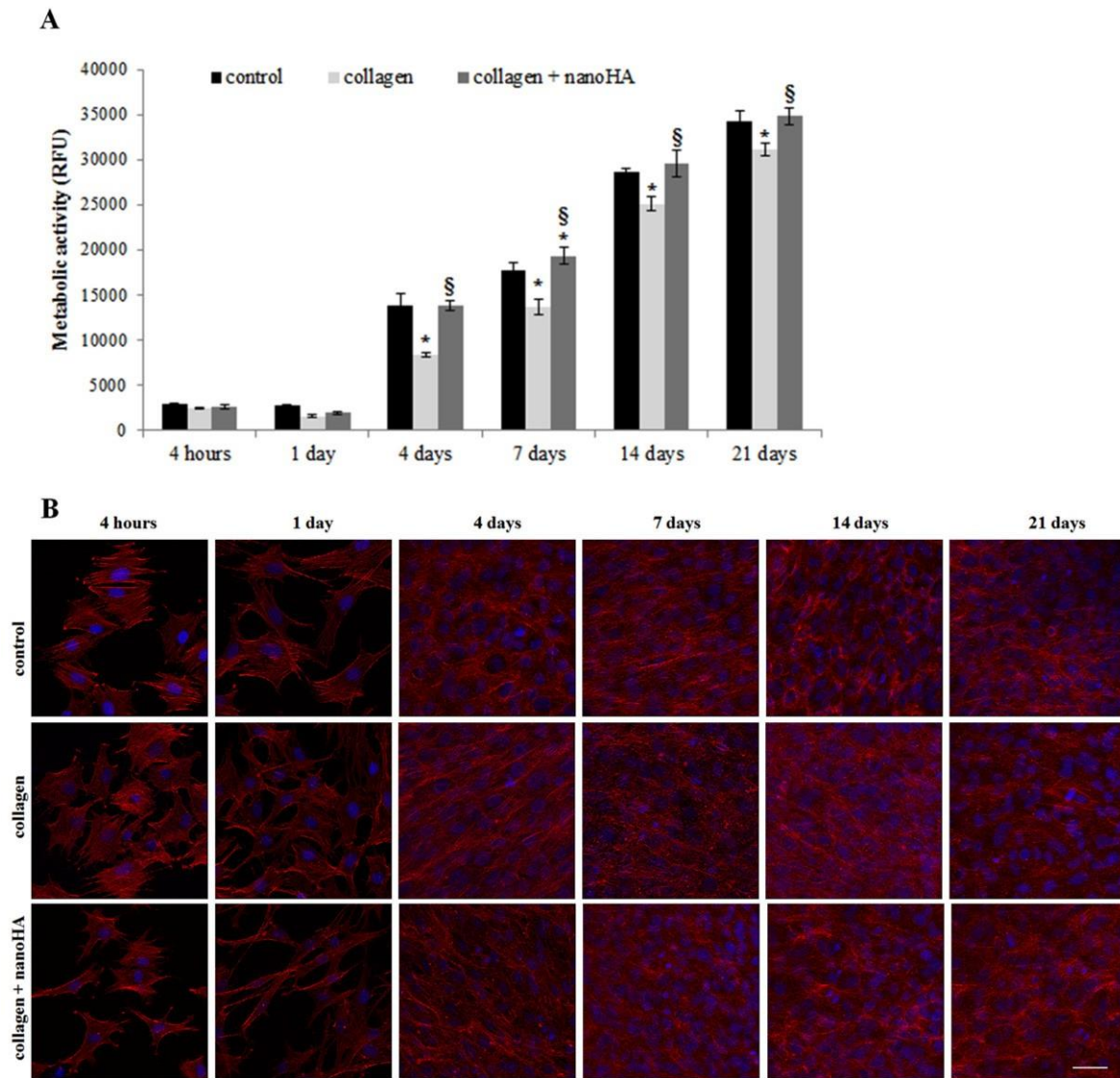


Figure 6. Metabolic activity (A) and morphology and cytoskeletal organization (B) of MC3T3-E1 cells cultured on the electrospun collagen nanofibers and the collagen–nanoHA composites obtained using the simultaneously electrospinning and electrospraying techniques versus time. In (A) the results are expressed in terms of relative fluorescence units (RFU); in (B) F-actin is indicated in red while the cells' nuclei were counterstained in blue with DAPI dye. MC3T3-E1 cells cultured on coverglasses coated with PDL were used as the control. Values are the average  $\pm$  SD of six cultures. \* indicates a statistically significant difference from the control cultures. \$ indicates a statistically significant difference from the cultures grown on the electrospun collagen nanofibers ( $p \leq 0.05$ ).

diameter of the collagen fibers obtained in this study is quite low when compared previous studies, can be attributed to the origin of the collagen, its concentration and most likely the type of solvents used and their  $v/v^{-1}$  % which are distinct from all the other studies. Figure 3((A)(iii)) shows a representative SEM image of the collagen–nanoHA composites obtained using simultaneous electrospinning and electrospraying techniques. A random arrangement of collagen nanofibers and irregular structures of nanoHA incorporated between them can be observed.

In this nano-network either collagen or nanoHA is accessible, resembling the ECM organization of bone tissue. Until now, all collagen–HA composites obtained by electrospinning were prepared from a mixture of collagen and hydroxyapatite. As a consequence, the composite surface is

covered with collagen or HA, preventing direct cell/protein contact with both organic and inorganic components [15, 33, 43, 44]. The cross-linking procedure did not affect the morphological arrangement of the electrospun meshes.

The thicknesses of the collagen–HA biocomposites before and after chemical cross-linking were determined based on SEM images, allowing the calculation of the average values  $326 \pm 115$  nm and  $376 \pm 154$  nm, respectively. There is no statistically significant difference between the latter values, showing that the cross-linking procedure did not alter the physical structure proprieties in terms of thickness.

AFM studies confirmed the nanoscale dimensions of the collagen fibers, confirming the unprecedented resolution achieved with respect to the methodologies used thus far [10, 14, 18, 45, 46]. Moreover, the AFM images presented in



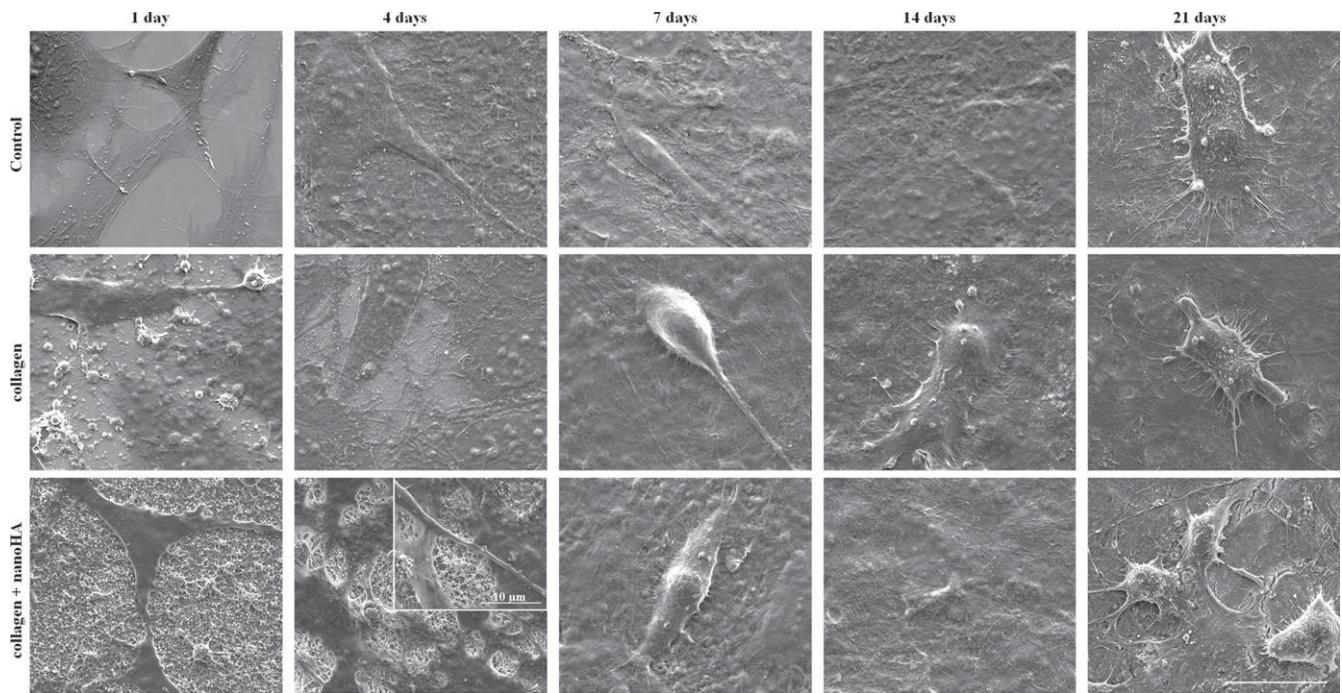


Figure 7. SEM images of MC3T3-E1 cells cultured on the electrospun collagen nanofibers and the collagen–nanoHA composites obtained using the simultaneous electrospinning and electro spraying techniques versus time. MC3T3-E1 cells cultured on coverglasses coated with PDL were used as control.

figures 4(A), (B) reveal a three-dimensional arrangement of collagen nanofibers. The ability of phase imaging AFM to distinguish samples with different surface viscoelastic properties enabled the visualization of the nanoHA agglomerates between the collagen nanofibers (figure 4((B)(ii))). Young's modulus ( $E$ ) of uncross-linked collagen nanofibers, cross-linked collagen nanofibers and collagen–HA composite (figure 5) was evaluated through a nanoindentation test. The cross-linking method and even the presence of nanoHA in the collagen–HA composite did not significantly affect the elastic modulus as shown in figure 5 [47]. The Young's moduli measured in this work were between 0.3 GPa and 2 GPa, which are lower than the values reported in Wenger *et al* but identical to those reported by Heim *et al* [48, 49].

### 3.2. MC3T3-E1 morphology and metabolic activity

The influence of both materials on MC3T3-E1 cell performance in terms of cell metabolic activity, cell distribution and morphology was investigated over a long period of cell culture, 21 days, with time points at 4 h and 1, 4, 7, 14 and 21 days. The pattern of metabolic activity in all the substrates was an increase with time of culture, indicating that both the collagen and biocomposite constructs presented a non-cytotoxic effect and had the ability to support osteoblast cell adhesion (figure 6(A)). Nevertheless, the metabolic activity of the osteoblasts cultured on the electrospun pure collagen nanofibers revealed lower values compared to the control samples and the biocomposite constructs at the latter culture time points (4, 7, 14 and 21 days). The inclusion of nanoHA agglomerates on type I collagen mesh induced proliferation of

MC3T3-E1 osteoblasts after 4 days of cell culture. The calcium ions seem to promote the adhesion of bone cells and stimulate its subsequent activity, as suggested by other authors [43, 44]. The analysis of cell metabolic activity at day 7 also suggests an increase of cell number on the nanostructured biocomposites. Once population capacity was reached, we hypothesize that a small number of cells might go through apoptosis as part of the regular cell life cycle, nevertheless metabolic activity on the control and electrospun biocomposites never ceased to grow, reaching identical values.

The cell distribution and morphology of MC3T3-E1 on the materials were followed by SEM and confocal imaging at the different time points of the cell culture, the results being in accordance with the metabolic activity data. At 4 h of cell culture, MC3T3-E1 cells were attached and were spread out across the surface, demonstrating a characteristic elongated shape with a fusiform fibroblastic appearance (figures 6(B) and 7). In particular, in figure 7 it is interesting to observe that the MC3T3-E1 cells cultured on the collagen–HA constructs seem to interact with both the organic and inorganic components without any preference. They completely adhered to the surface, closely binding the filopodia to the substrates and reaching a fusion state, making it difficult to distinguish, at some points, between parts of the cell (filopodia, products secreted by cells and their ECM) and the substrate material (meshes of collagen nanofibers and HA agglomerates). A compact film of cells was formed after 4 days of cell culture, rendering it almost impossible to observe individual cells among so many others widespread in several cell layers.



#### 4. Conclusion

In this work a novel composite based on collagen nanofibers and nanoHA agglomerates was successfully obtained using co-electrospinning–electrospraying. The collagen integrity as well as the nanoscale dimensions of both the biocomposite components (collagen and nanoHA) were preserved as confirmed by FT-IR spectra, and SEM and AFM image analysis. In the development of the construct, water-based solvents (ethyl acetate, acetic acid and water) and non-collagen denaturing conditions were applied. The diameters of the electrospun collagen nanofibers, estimated from the SEM images to range between 10 and 100 nm, are far below those stated in the literature, thus offering a roadmap to obtain a further level of biomimicry in matrix design strategies. This novel construct allows cells access to both collagen nanofibers and HA crystals as happens in the natural bone micro- and nano-environments. Regarding cellular interactions, these structures were cytocompatible and able to withstand adhesion and growth of MC3T3-E1 osteoblasts in the long-term. This new collagen nanofiber–nanoHA composite is an excellent biomaterial candidate for bone tissue regeneration with conditions similar to human ECM, as well as in biomedical applications in small bone defects and for coating the surfaces of other materials with a mechanical support function.

#### Acknowledgements

The authors would like to thank the financial support for this work from NR's PhD grant (Ref. SFRH/BD/69686/2010) provided by Fundação para a Ciência e a Tecnologia (FCT). Also, the provision of nanoHA (nanoXIM) by FLUIDI-NOVA, S.A. (Maia-Portugal) and collagen by Kensey Nash (USA) is gratefully acknowledged. The authors thank María Gómez Lázaro for technical assistance in Confocal imaging and Carlos Silva for technical assistance in the laboratory set-up used for the simultaneous electrospinning and electrospraying techniques. This work was financed by FEDER funds through the Programa Operacional Factores de Competitividade—COMPETE and by Portuguese funds through FCT—Fundação para a Ciência e a Tecnologia in the framework of the project PEst-C/SAU/LA0002/2013.

#### References

- [1] Al-Munajjed A A *et al* 2009 Development of a biomimetic collagen-hydroxyapatite scaffold for bone tissue engineering using a SBF immersion technique *J. Biomed. Mater. Res. B Appl. Biomater.* 90 584–91
- [2] Curtin C M *et al* 2012 Innovative collagen nano-hydroxyapatite scaffolds offer a highly efficient non-viral gene delivery platform for stem cell-mediated bone formation *Adv. Mater.* 24 749–54
- [3] Manuel C M, Foster M, Monteiro F J, Ferraz M P, Doremus R H and Bizios R 2003 Preparation and characterization of calcium phosphate nanoparticles *16th Int. Sym. on Ceramics in Medicine (Porto, Portugal)* (Zurich: Trans Tech) 903–6
- [4] Teixeira S, Fernandes H, Leusink A, Van Blitterswijk C, Ferraz M P, Monteiro F J and De Boer J 2010 *In vivo* evaluation of highly macroporous ceramic scaffolds for bone tissue engineering *J. Biomed. Mater. Res. A* 93 567–75
- [5] Wahl D A and Czernuszka J T 2006 Collagen-hydroxyapatite composites for hard tissue repair *Eur. Cell Mater.* 11 43–56
- [6] Bhardwaj N and Kundu S C 2010 Electrospinning: a fascinating fiber fabrication technique *Biotechnol. Adv.* 28 325–47
- [7] Shi J J, Votrubá A R, Farokhzad O C and Langer R 2010 Nanotechnology in drug delivery and tissue engineering: from discovery to applications *Nano Lett.* 10 3223–30
- [8] Jarvinen T A H, Jarvinen T L N, Kannus B B, Jozsa L and Jarvinen M 2004 Collagen fibres of the spontaneously ruptured human tendons display decreased thickness and crimp angle *J. Orthop. Res.* 22 1303–9
- [9] Yang L, Fitie C F C, van der Werf K O, Bennink M L, Dijkstra P J and Feijen J 2008 Mechanical properties of single electrospun collagen type I fibers *Biomaterials* 29 955–62
- [10] Chen R, Huang C, Ke Q F, He C L, Wang H S and Mo X M 2010 Preparation and characterization of coaxial electrospun thermoplastic polyurethane/collagen compound nanofibers for tissue engineering applications *Colloid Surface B* 79 315–25
- [11] Chen Z G, Mo X M, He C L and Wang H S 2008 Intermolecular interactions in electrospun collagen-chitosan complex nanofibers *Carbohydr. Polym.* 72 410–8
- [12] Chen Z G, Wang P W, Wei B, Mo X M and Cui F Z 2010 Electrospun collagen-chitosan nanofiber: a biomimetic extracellular matrix for endothelial cell and smooth muscle cell *Acta Biomater.* 6 372–82
- [13] Guo F *et al* 2011 A novel amperometric hydrogen peroxide biosensor based on electrospun Hb-collagen composite *Colloid Surface B* 86 140–5
- [14] Hartman O *et al* 2009 Microfabricated electrospun collagen membranes for 3D cancer models and drug screening applications *Biomacromolecules* 10 2718
- [15] Hild N *et al* 2011 Two-layer membranes of calcium phosphate/collagen/PLGA nanofibers: *in vitro* biomineralisation and osteogenic differentiation of human mesenchymal stem cells *Nanoscale* 3 401–9
- [16] Liu S J, Kau Y C, Chou C Y, Chen J K, Wu R C and Yeh W L 2010 Electrospun PLGA/collagen nanofibrous membrane as early-stage wound dressing *J. Membrane. Sci.* 355 53–9
- [17] Matthews J A, Wnek G E, Simpson D G and Bowlin G L 2002 Electrospinning of collagen nanofibers *Biomacromolecules* 3 232–8
- [18] Zhong S P, Teo W E, Zhu X, Beuerman R W, Ramakrishna S and Yung L Y L 2006 An aligned nanofibrous collagen scaffold by electrospinning and its effects on *in vitro* fibroblast culture *J. Biomed. Mater. Res. A* 79A 456–63
- [19] Zhong S P, Teo W E, Zhu X, Beuerman R, Ramakrishna S and Yung L Y L 2007 Development of a novel collagen-GAG nanofibrous scaffold via electrospinning *Mat. Sci. Eng. C-Bio. S.* 27 262–6
- [20] Cao D *et al* 2011 Cell adhesive and growth behavior on electrospun nanofibrous scaffolds by designed multifunctional composites *Colloid Surface B* 84 26–34
- [21] Choi J S, Lee S J, Christ G J, Atala A and Yoo J J 2008 The influence of electrospun aligned poly (epsilon-caprolactone)/collagen nanofiber meshes on the formation of self-aligned skeletal muscle myotubes *Biomaterials* 29 2899–906
- [22] Wang G L, Hu X D, Lin W, Dong C C and Wu H 2011 Electrospun PLGA-silk fibroin-collagen nanofibrous scaffolds for nerve tissue engineering *In Vitro Cell Dev-An* 47 234–40
- [23] Anderson J M, Rodriguez A and Chang D T 2008 Foreign body reaction to biomaterials *Semin. Immunol.* 20 86–100

- [24] Dawes E and Rushton N 1994 The effects of lactic acid on PGE2 production by macrophages and human synovial fibroblasts: a possible explanation for problems associated with the degradation of poly(lactide) implants? *Clin. Mater.* 17 157–63
- [25] Yang Z X *et al* 2010 Easy preparation of SnO<sub>2</sub>@carbon composite nanofibers with improved lithium ion storage properties. *J. Mater. Res.* 25 1516–24
- [26] Zeugolis D I *et al* 2008 Electro-spinning of pure collagen nanofibres—just an expensive way to make gelatin? *Biomaterials* 29 2293–305
- [27] Dong B, Arnoult O, Smith M E and Wnek G E 2009 Electrospinning of collagen nanofiber scaffolds from benign solvents *Macromol. Rapid Comm.* 30 539–42
- [28] Foltran I, Foresti E, Parma B, Sabatino P and Roveri N 2008 Novel biologically inspired collagen nanofibers reconstituted by electrospinning method *Macromol. Symp.* 269 111–8
- [29] Liu T, Teng W K, Chan B P and Chew S Y 2010 Photochemical crosslinked electrospun collagen nanofibers: synthesis, characterization and neural stem cell interactions *J. Biomed. Mater. Res.* A 95A 276–82
- [30] Zhou J A, Cao C B, Ma X L and Lin J 2010 Electrospinning of silk fibroin and collagen for vascular tissue engineering *Int. J. Biol. Macromol.* 47 514–9
- [31] Buttafoco L *et al* 2006 Electrospinning of collagen and elastin for tissue engineering applications *Biomaterials* 27 724–34
- [32] Teixeira S, Yang L, Dijkstra P J, Ferraz M P and Monteiro F J 2010 Heparinized hydroxyapatite/collagen three-dimensional scaffolds for tissue engineering *J. Mater. Sci.-Mater. M.* 21 2385–92
- [33] Teng S H, Lee E J, Wang P and Kim H E 2008 Collagen/hydroxyapatite composite nanofibers by electrospinning *Mater. Lett.* 62 3055–8
- [34] Vrana N E *et al* 2007 EDC/NHS cross-linked collagen foams as scaffolds for artificial corneal stroma *J. Biomat. Sci.-Polym.* E 18 1527–45
- [35] Wissink M J B *et al* 2001 Immobilization of heparin to EDC/NHS-crosslinked collagen. characterization and *in vitro* evaluation *Biomaterials* 22 151–63
- [36] Francis L, Venugopal J, Prabhakaran M P, Thavasi V, Marsano E and Ramakrishna S 2010 Simultaneous electrospin-electrosprayed biocomposite nanofibrous scaffolds for bone tissue regeneration *Acta Biomater.* 6 4100–9
- [37] Gupta D, Venugopal J, Mitra S, Dev V R G and Ramakrishna S 2009 Nanostructured biocomposite substrates by electrospinning and electrospraying for the mineralization of osteoblasts *Biomaterials* 30 2085–94
- [38] VanLandingham M R, Villarrubia J S, Guthrie W F and Meyers G F 2001 Nanoindentation of polymers: an overview *Macromol. Symp.* 167 15–43
- [39] Song J H, Kim H E and Kim H W 2008 Production of electrospun gelatin nanofiber by water-based co-solvent approach *J. Mater. Sci.-Mater. M.* 19 95–102
- [40] Chang M C and Tanaka J 2002 FT-IR study for hydroxyapatite/collagen nanocomposite cross-linked by glutaraldehyde *Biomaterials* 23 4811–8
- [41] Fernandes L L, Resende C X, Tavares D S, Soares G A, Castro L O and Granjeiro J M 2011 Cytocompatibility of chitosan and collagen–chitosan scaffolds for tissue engineering *Polimeros* 21 1–6
- [42] Ribeiro C C, Gibson I and Barbosa M A 2006 The uptake of titanium ions by hydroxyapatite particles—structural changes and possible mechanisms *Biomaterials* 27 1749–61
- [43] Song W, Markel D C, Wang S X, Shi T, Mao G Z and Ren W P 2012 Electrospun poly(vinyl alcohol)–collagen–hydroxyapatite nanofibers: a biomimetic extracellular matrix for osteoblastic cells *Nanotechnology* 23 11
- [44] Venugopal J, Low S, Choon A T, Kumar T S S and Ramakrishna S 2008 Mineralization of osteoblasts with electrospun collagen/hydroxyapatite nanofibers *J. Mater. Sci.-Mater. M.* 19 2039–46
- [45] Carlisle C R, Coulais C and Guthold M 2010 The mechanical stress–strain properties of single electrospun collagen type I nanofibers *Acta Biomater.* 6 2997–3003
- [46] Song W, Markel D C, Jin X, Shi T and Ren W P 2012 Poly(vinyl alcohol)/collagen/hydroxyapatite hydrogel: properties and *in vitro* cellular response *J. Biomed. Mater. Res.* A 100A 3071–9
- [47] Duan X and Sheardown H 2005 Crosslinking of collagen with dendrimers *J. Biomed. Mater. Res.* A 75A 510–8
- [48] Heim A J, Matthews W G and Koob T J 2006 Determination of the elastic modulus of native collagen fibrils via radial indentation *Appl. Phys. Lett.* 89 18
- [49] Wenger M P E, Bozec L, Horton M A and Mesquida P 2007 Mechanical properties of collagen fibrils *Biophys. J.* 93 1255–63